Hittite Journal of Science and Engineering, 2014, 1 (1) , 13-20
ISSN NUMBER: 2149-2123
DOI: 10.17350/HJSE19030000003

Thermal Performance and Pressure Drop of Different Pin-Fin Geometries

Isak Kotcioglu[1], Gokhan Omeroglu[1] and Sinan Caliskan[2,*]
[1] Atatürk University, Department of Mechanical Engineering, Erzurum, TURKEY
[2] Hitit University, Department of Mechanical Engineering, Corum, TURKEY

ABSTRACT

The purpose of this study is to show the performance of hexagonal, square and cylindrical pin-fin arrays in improving heat transfer. In the present study, the thermal performance and pressure drop of the pin-fin heat exchanger are studied. The heat exchanger consists of cylindrical, hexagonal and square pin-fins. These types of pin-fins are capable of producing beneficial effects in transport enhancement and flow control. The pin-fins were arranged in an in-line manner. The relative longitudinal pitch (S_L/D=2), and the relative transverse pitch were kept constant (S_T/D=2). Air and water are used as working fluids in shell side and tube side, respectively. The inlet temperatures of air are between 50 and 90° C. The cold water entering the heat exchanger at the inner channel flows across the fin and flows out at the inner channel. Such pin-fins show potential for enhancing the heat transfer rate in pin-fin cross flow heat exchangers.

Article History:
Received: 2014/09/12
Accepted: 2014/12/22
Online: 2014/12/31

***Correspondence to**: Sinan Calıskan,*
Hitit University, Faculty of Engineering,
Department of Mechanical Engineering,
Corum, Turkey
Tel: +90 (364) 227-4533
Fax: +90 (364) 227-4535
E-Mail: sinancaliskan2000@yahoo.com

Key Words:
Thermal performance; Pressure drop; Cylindrical, Hexagonal and square ins

NOMENCLATURE

A	: Cross-sectional area of the test channel [m^2]
A_{total}	: Total heat dissipation area of pin-fins [m^2]
A_{base}	: Bottom area of the test channel [m^2]
A_f	: Fin surface area on one side of an exchanger [m^2]
A_o	: Minimum free-flow area [m^2]
D	: Pin-fins diameter [m]
D_{ch}	: Hydraulic diameter of the channel [m]
d_o	: Outer diameter of the tube [m]
d_i	: Internal diameter of the tube [m]
h	: Length of the hexagonal pin-fins [m]
k	: Conductivity [W/mK]
h_{av}	: Average convective heat transfer coefficient [W/m^2K]
L_1	: Height of the test section [m]
L_2	: Length of the test section [m]
L_3	: Width of the test section [m]
N_t	: Total number of pin-fins
N_f	: Number of pin-fins per unit length
Nu_D	: Pin-fin Nusselt number
Q	: Heat transfer rate [W]
s	: Length of the square pin-fins [m]
T	: Temperature [K]
t	: Distance between the pin-fins [m]
T_s	: Average surface temperature [K]
U	: Volumetric average fluid velocity [m/s]
S_L/D	: Relative longitudinal pitch
S_T/D	: Relative transverse pitch
ΔP	: Pressure drop [N/m^2]

Greek symbols

δ	: Plate thickness [m]
μ	: Fluid dynamic viscosity [kg /ms]
ρ	: Air density [kg/m^3]

Dimensionless numbers

f	: Friction factor
Re_D	: Pin-fin Reynolds number

Subscripts

c	: Circular
h	: Hexagonal
s	: Square
in	: Inlet
out	: Outlet
x, y	: Spanwise and streamwise direction, respectively

INTRODUCTION

Needs for small-size and light-weight heat exchanger devices in power, process, computer and aerospace industries have resulted heat transfer surfaces. In order to enhance heat transfer between the flowing fluid and closely-spaced pin fins, in the case of pin-fin heat exchangers, pin-fins can be mounted on the channel surfaces.

Jeng et al. [1] experimentally studied the pressure drop and heat transfer of a square pin-fin array in a rectangular channel by using the transient single-blow technique. The in-line square pin-fin array has smaller pressure drop than the in-line circular pin-fin array. The optimal inter-fin pitches of in-line square pin fin arrays are Xt = *2* and X_L = *1.5*, its Nu_D^* is around 20% higher than that of the in-line circular pin-fin array. Vanfossen [2] studied heat transfer by short pin-fins in staggered arrangements. According to their results, longer pin-fins transfer more heat than shorter pin-fins and the array-averaged heat transfer with eight rows of pin-fins slightly exceeds that with only four rows. Their results also established that the average heat transfer coefficient on the pin surface is around 35% larger than that on the end walls.

Grannis and Sparrow [3] used the experiments to verify the accuracy of a numerical simulation of fluid flow through a diamond-shaped pin-fin array. They provided a correlation between the friction factor and the Reynolds number based on the results of numerical calculations.

Young et al. [4] experimentally examined the performs of pin-fin heat sinks having circular, elliptic, and square cross-section. The effect of pin-fin density on the heat transfer performance was examined. The elliptic pin-fin shows the lowest pressure drops. For the same surface area at a fixed pumping power, the elliptic pin-fin possesses the smallest thermal resistance for the staggered arrangement. Sparrow et al. [5] investigated pin-fin arrays both numerically and experimentally. The effects of length to diameter, array geometry, entrance length, and pin-fin shape have been reported.

Effects of height and width of hexagonal pin-fins, stream-wise and span-wise distances between pin-fins, and flow velocity on thermal resistance and pressure drop characteristics were investigated using Taguchi experimental design method by Yakut et al. [6]. They also determined the temperature distribution within the selected pin-fins. Chen et al. [7] carried out experiments regarding heat transfer and pressure drop coefficients in a rectangular duct with drop-shaped pin-fins. They reported the Nusselt number for a channel with drop-shaped pin-fins to be slightly higher than those of circular ones. Similarly, they also found out that the pressure drop of drop-shaped pin-fins is 42-51% less than that of circular ones.

Ricci and Montelpare [8] aimed to evaluate the convective heat transfer coefficient, i.e. the Nusselt number, of short pin-fins cooled by means of water in forced convection. In particular the work is focused on the geometry (circular, square, triangular, rhomboidal) shape effect for three pin-fins assembled in line and the thermal analysis is performed by using a quantitative infrared method developed in a previous work. The thermal analysis is related to ink flow visualizations in order to better understand the effects of the main flow field on the thermal exchange capacities of every pin-fin inside the line. Nusselt numbers and flow structural characteristics are presented by Won et al. [9] for a stationary channel with an aspect ratio of 8 and a staggered array of pin-fins between two of the surfaces. Local Nusselt numbers, measured on one end wall, are highest beneath primary and secondary horseshoe vortices located just upstream of individual pin-fins.

Hwang and Lu [10] made a study which is especially unique because three pin-fin configurations, each arranged in a staggered array, are considered in a trapezoidal duct, both with and without lateral flow ejection. Wang et al. [11]presented flow visualization and frictional results of enlarged pin-fin and tube heat exchangers with and without the presence of vortex generators. Two types of vortex generators and plain pin-fin geometry were examined in the study. Compared to the plain pin-fin geometry, the penalty of additional pressure drops of the proposed vortex generators is relatively insensitive to change of Reynolds number. As mentioned above, numerous works have been reported concerning the heat transfer and pressure drop for different pin-fin configurations.

Optimal spacing of a pin-fin in the span-wise and stream-wise directions has been determined by Kotcioglu et al. [12]. The experimental results showed that the use of hexagonal pin-fins, compared to square and cylindrical pin-fins, may lead to an advantage on the basis of heat transfer enhancement. The optimal inter-fin pitches are provided based on the largest Nusselt number under the same pumping power, while the optimal inter-fin pitches of hexagonal pin-fins were $S_T/D=2$ and $S_L/D= 2.8$.

The present study is an investigation of heat transfer characteristics and pressure drop in a channel with hexagonal, square and cylindrical pin-fins attached to upper and lower plates in an in-line arrangement. Effects of various relevant parameters on the heat transfer and pressure drop characteristics for different geometrical parameters are considered. According to the obtained results, heat

transfer and differences among the channel f factor of the pin-fins are basically because of the geometrical shapes of the pin-fins, causing different flow patterns and vortices. Understanding these kinds of pin-fins, which are used widely in industry, is believed to give a rich contribution to elucidation of the phenomena in heat exchangers used in different applications.

EXPERIMENTAL

The channel flow experimental rig is shown in Figure l. The rig consisted of a closed rectangular channel with a removable test section (16), blower (13), a data acquisition system (11), U-type manometer (8), heater (2), and thermocouples (17). The flow channel was constructed of wood of 20 mm thickness, had an internal cross section of 0.098 m width and 0.014 m height with a wall thickness of 0.01 m. Total length of the channel was 2 m. The system was operated in suction mode and positioned horizontally. A flow straightener (1) was fitted immediately after the inlet of the channel. In order to minimize the heat loss, the other surfaces of the heater were insulated by a combination of a 12 mm thick asbestos layer and a 20 mm thick glass. The thermostat (3), of which only the upper outside surface of the channel was heated, was located 0.25 m downstream of the flow straightener. Test section (16) was fitted 1.5 mm downstream of the inlet of the flow channel. The flow channel consisted of a wooden channel. The outlet of the flow channel length was at 0.90 m. The base plates of the test surface were made from two plates with aluminium alloy (ρ=2710 kg/m^3) as the rectangular channel of 5 mm thickness, 14 mm height, 98 mm width, and 130 mm length. Various type of pin-fins, which were made of the same aluminium material as the base plate, were attached between the bottom and upper surface of the base plates Figure 2 (a, b). Thermal glue was applied between the plate and the pin-fins for a better contact. The number of pin-fins can be adjusted to suit the required spacing between the pin-fins in the stream-wise direction. Twelve thermocouples were equally spaced along the base and top plate between the pin-fins for measurement of the bottom and top plate temperatures. They were equally spaced and in all cases positioned in the spaces between the pin-fins. Four thermocouples were used to measure the temperatures of the inlet and outlet of the air and water, respectively.

Analog signals from the experimental system were fed to the data acquisition card. All thermocouples were separately calibrated before being used in the experiments. While the air flow is passing from the horizontal direction of the channels, the water is passing from the vertical direction (see Figure 2a). The air transfers its heat to the water during this process. The pressure drop was determined using a glass tube U type manometer. The air flow temperature was controlled by a thermostat. Inlet temperature of the water

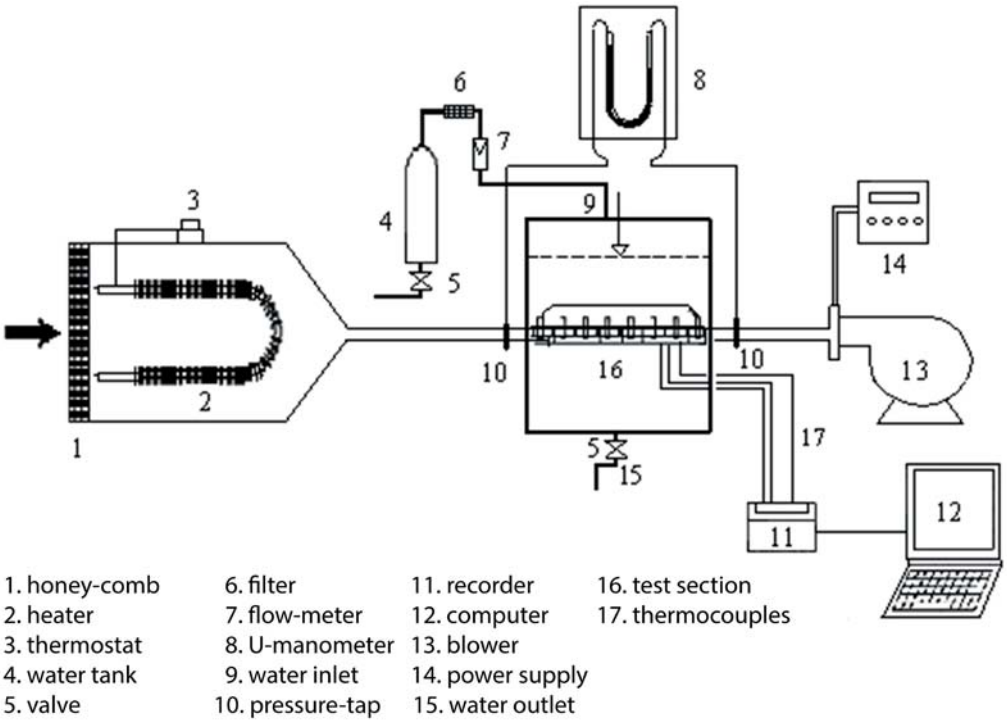

Figure 1. Schematic of experimental apparatus

was held between 17-20 °C. In the experiments, the duration to reach steady-state conditions was about 0.5-1 hour, depends on experimental conditions. The arrangement of the pin-fins on the test section is illustrated in Figure 2b.

Geometrical characteristics of the pin-fins are given Table 1.

Table 1. Geometrical characteristics of the pin-fins

	$A_o(m^2)$	$A_p(m^2)$	$A_f(m^2)$	$A(m^2)$
Hexagonal	*0.000612*	*0.03175*	*0.0000880*	*0.03183*
Square	*0.000612*	*0.03175*	*0.0001436*	*0.03189*
Circular	*0.000612*	*0.03175*	*0.0001356*	*0.03188*

Distance between pin-fins and number of pin-fins are given Table 2.

Table 2. Distance between pin-fins and number of pin- fins

Configuration	*Arrangement*	$S_L/D=2$ and $S_T/D=2$		
		Nx	*Ny*	$N_{tot.}$
Hexagonal	*In- line*	*6*	*8*	*48*
Square	*In- line*	*6*	*8*	*48*
Circular	*In- line*	*6*	*8*	*48*

Geometrical properties of heat exchanger surface

The basic core geometry for an idealized single-pass cross-flow heat exchanger with an inline pin-fin arrangement is shown in Figure 2b. Total number of pin-fins, N_t is given as;

$$N_t = (L_2 L_3)/S_T S_L \quad (1)$$

The total heat transfer area A consists of the area associated with the exposed pin-fins and header plates (primary surface area) A_p, and pin-fins (secondary surface area) A_f. For the circular, square and hexagonal fin, geometrical characteristics concerning the fin-tube outside surface are given as;

$$A_p = \pi d_o (L_1 - \delta N_f L_1) N_t + 1(L_2 L_3 - (\pi d_o^2/4) N_t) \quad (2)$$

Here ρ, is the plate thickness and N_f is the number of pin-fins per unit length. For the circular, square and hexagonal pin-fin, (secondary surface area) A_f is given respectively by;

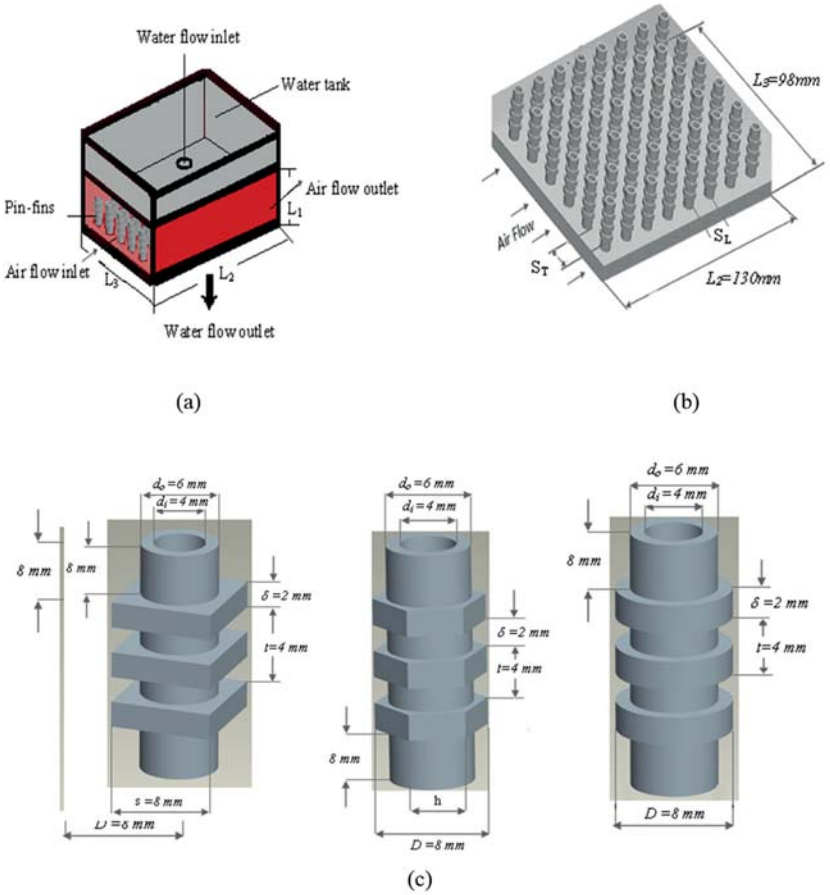

Figure 2. Shown are a) test section, b) upper view of the arrangement over the plate of hexagonal pin-fins, c) square, hexagonal, circular pin-fins, respectively.

$$A_{fc}=[2\pi(D^2-d_o^2)/4 + (\pi D\delta)]\ N_t N_f L_1 \quad (3)$$

$$A_{fs}=[s^2- (\pi d_o^2)/4 + (4s\delta)]\ N_t N_f L_1 \quad (4)$$

$$A_{fh}=[(2.59h^2- (\pi d_o^2/4) + (6h\delta)]\ N_t N_f L_1 \quad (5)$$

where D is the pin-fin diameter, d_0 is an outer diameter of the tube, δ is plate thickness, s is length of the square pin-fin and h is length of the hexagonal pin-fin. Total heat transfer area is then

$$A=A_p+A_f \quad (6)$$

Minimum free-flow area for inline arrangement is given by,

$$A_0=[(S_T - d_o)L_1 - (D-d_0)\ \delta N_f L_1](L_3/S_T) \quad (7)$$

Data reduction

The heat transfer modes of interest for the present system are conduction, convection and radiation through the air and water. The magnitude of each mode depends on the temperature of the pin-fin array's base, the assembly material and pin-fin geometry. Thus the heat balance equation for the whole system can be expressed as follows:

$$Q_{total}= Q_{conv.} + Q_{rad.} + Q_{loss} \quad (8)$$

In similar studies [13-16], it was reported that the total radiative heat-losses from a similar test surface would be about 0.5% of the total electrical heat-input. Therefore, the radiative heat loss could be neglected. Using these findings, together with the fact that the test section was well insulated and the readings of the thermo junction, placed at the outer surface of the heating section, was nearly equal to the ambient temperature. Then one could assume with some confidence that the last two terms of Eq. (8) may be ignored. Then, the Eq. (8) is reduced to

$$Q_{total} = Q_{conv.} \quad (9)$$

The steady-state convection heat transfer from the test section by convection can be expressed as,

$$Q_{conv.} = h_{av}A[\bar{T}_s - ((\bar{T}_{out}+\bar{T}_{in})/2)] \quad (10)$$

where $\bar{T}_s$ is average surface temperature of the base plate for the pin-fin assembly of the heat exchanger. $\bar{T}_{in}$ and $\bar{T}_{out}$ are the mean temperatures of the air flow at the inlet and the outlet, respectively. In all the calculations, the values of the thermo-physical properties of the air were obtained at the average bulk mean temperature from $\bar{T}_s = (\bar{T}_{out}+\bar{T}_{in})/2$. Either the projected or the total area of the test surface can be taken as the surface area in the calculations.

In the present experimental investigation, two types of Reynolds number were used to characterize the flow conditions. One is a Reynolds number based on the mean velocity (U) and the hydraulic diameter of the channel (D_{ch}) expressed as

$$Re=(\rho D_{ch} U)/\mu \quad (11)$$

Re is the channel Reynolds number. The other one is based on the maximum velocity through the pin-fins and the thickness of the pin-fins.

$$Re_D= (\rho D U_{max})/\mu \quad (12)$$

Re_D has been widely used as pin-fin Reynolds number in many pin-fin heat transfer studies. U_{max} is the maximum velocity through the fins and is given by

$$U_{max}=(A/(A-A_f)U) \quad (13)$$

where A is the cross-sectional area of the test channel and A_f is the frontal area of the pin-fins. In order to compare the results with those of other researches, this section applies the pin-fins Nusselt number Nu_D and $Re_D(U_{max}/U)$ to elucidate the relationship between the heat transfer and the maximum velocity of pin-fin array with various inter-fin pitches. For the present experimental setup, the values of $A/(A-A_f)$ are given in Table 3.

Table 3. Values of $A/(A-A_f)$ for $S_L/D=2$.

S_L/D	Hexagonal	Square	Circular
2	1.00277	1.00452	1.00427

The average Nusselt number is represented by pin-fin Nusselt number

$$Nu_D= (h_{av}D/k) \quad (14)$$

where is the average convective heat transfer coefficient and is the thermal conductivity of air. The friction factor (f) is defined as follows,

$$f=\Delta P/((L_2/D_{ch})\rho(U^2/2) \quad (15)$$

where is the density of air, the length of the test section, pressure drop, U average fluid velocity and D_{ch} channel hydraulic diameter.

Uncertainty analysis

By using the estimation method of Kline and McClintock [17] maximum uncertainty of mass flow rate was ±2.3%. The uncertainty in the pressure was 6.5%. The experimental results herein revealed that the uncertainties in the Reynolds number and Nusselt number were ±6.8% and ±7%, respectively. The individual contributions to the uncertainties for each of the measured physical properties are summarized in Table 4. A detailed error analysis is made to estimate the W_R uncertainty arising from different independent variables from the following equation

$$W_R=[(\partial RW_1/\partial x_1)^2+ (\partial RW_2/\partial x_2)^2+.....+(\partial RW_n/\partial x_n)^2]^{1/2} \quad (16)$$

Table 4. Uncertainties in the values of the relevant variables

Variable	Uncertainty (%)
Velocity of the air, U	0.5
Mean Temperature, T	0.25
Pressure, P	6.5
Hydraulic diameter of the channel,	0.1
Voltage, V	0.1
Current, I	0.72
Dynamic viscosity of the air,	0.045
Thermal conductivity of the air, k	0.33
Density of the air,	0.007
Re	0.068
Nu	0.070
f	0.065

RESULTS

Figures 3-6 shows the variation of the average bottom and top plate temperatures with air Reynolds number for two inlet air temperatures (50 and 90°C). As expected, the heat transfer rate depends on the cooling capacity rate of inlet air temperatures. Therefore, the average bottom plate temperature decreases with increasing of Reynolds number. However, this effect tends to diminish as Reynolds number increases. As shown in Figure 3, the average bottom plate temperature depends on the supplied heat to the cylindrical, hexagonal and square pin-fins. In addition, average bottom plate temperatures at higher hexagonal are lower than those from lower ones. Due to higher surface area, heat transfer from the surface to the air increases. Therefore, cylindrical pin-fins give lower bottom plate temperatures. The average top plate temperatures are higher than bottom plates. As shown in Figures 3-6, hexagonal pin-fin arrays increase heat transfer more by increasing the flow turbulence than circular and square pin-fin arrays. The growth of recirculation zones promote the mixing of fluid in the boundary layer, thereby enhancing the convective heat transfer.

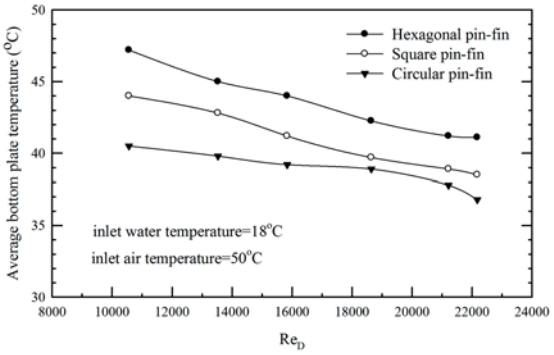

Figure 3. Variation of average bottom plate temperature with Reynolds number.

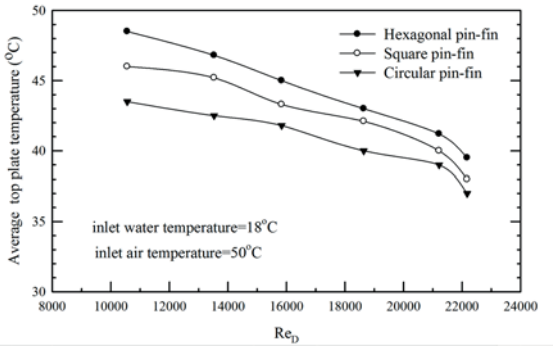

Figure 4. Variation of average top plate temperature with Reynolds number.

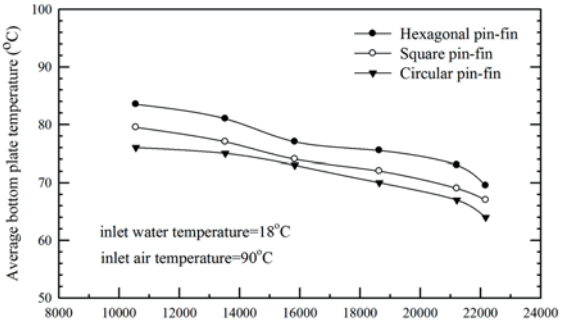

Figure 5. Variation of average bottom plate temperature with Reynolds number.

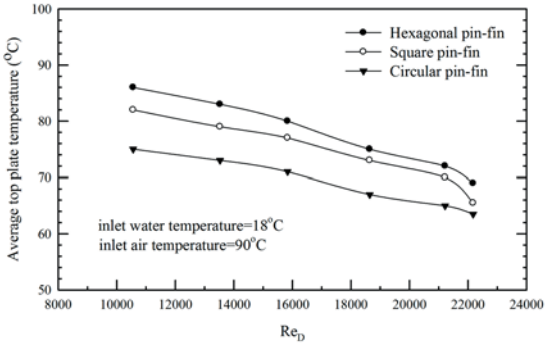

Figure 6. Variation of average top plate temperature with Reynolds number.

Figure 7 shows the variation of Nusselt number with air Reynolds number for square pin-fins for different inlet air temperatures. It can be seen that the Nusselt number tends to increases as air Reynolds number and inlet air temperatures are increased. For a given air Reynolds number, inlet air temperature has a significant effect on the Nusselt number.

Figure 8 shows the variation of the outlet air temperature with air Reynolds number for different pin-fins. Outlet air temperature tends to decrease as Reynolds number increases. As expected, when the Reynolds numbers are kept constant, pin-fins geometry has significant effect on the outlet air temperatures. Higher of fluid re-circulation or/and higher swirl flows change in the geometrical shapes, therefore the Nusselt number increases as shown in Figure 8.

Figure 9 depicts the friction factor (f) for the pin-fins as a function of the Reynolds number (Re_D). The circular pin–fins have smaller pressure drops than the hexagonal and square pin-fins. The results show that the pressure drop falls as Re number increases. These differences among the channel friction factor of the pin-fins are basically because of the geometrical shapes of the pin-fins causing different flow patterns and vortices.

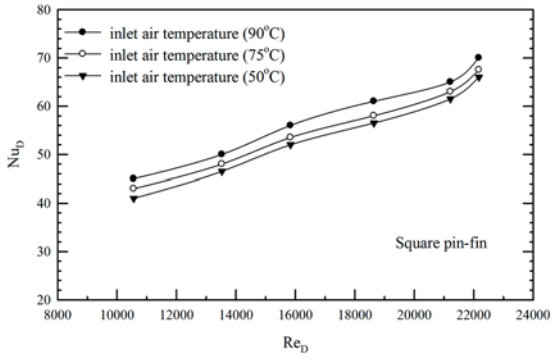

Figure 7. Variation of Nusselt number with Reynolds number for different inlet air temperatures.

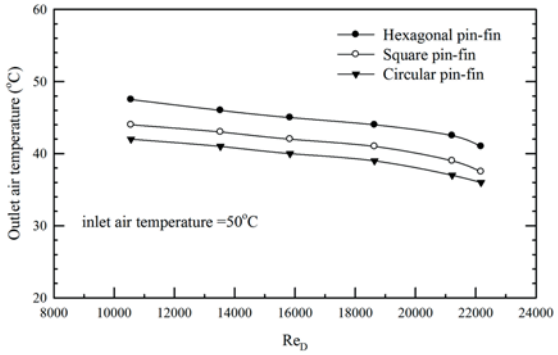

Figure 8. Variation of outlet air temperature with Reynolds number.

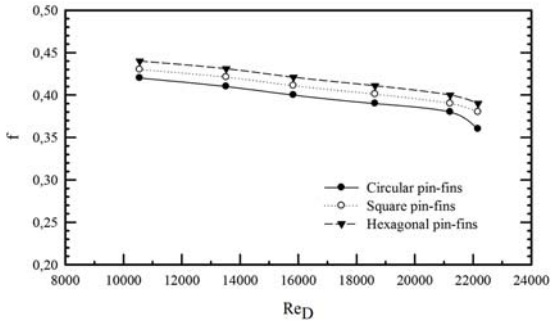

Figure 9. Duct friction factor as a function of Reynolds number.

CONCLUSIONS

Forced convection in a rectangular channel with various pin-fins geometries has been experimentally investigated. The pin-fins were inserted periodically into the rectangular channel. The effects of the geometrical parameters on the heat transfer and friction characteristics were determined. The following conclusions were drawn from the results of the present work:

- The average bottom and top plate temperatures decrease as air Reynolds number increases. The highest values of the bottom and top plate temperatures were obtained for the hexagonal geometry and 90°C inlet air temperature.
- The circular pin-fins array has a smaller pressure drop compared to the square and hexagonal pin-fins arrays.
- The Nusselt number increased with increasing inlet air temperature.

REFERENCES

1. Jeng TM, Tzeng SC. Pressure drop and heat transfer of square pin-fin arrays in in–line and staggered arrangements. International Journal of Heat and Mass Transfer 50 (2007) 2364–2375.

2. Vanfossen GJ. Heat transfer coefficients for staggered arrays of short pin-fins. Transactions of ASME, Journal of Heat Transfer 104 (1982) 268-274.
3. Grannis VB, Sparrow EM. Numerical simulation of fluid flow through an array of diamond-shaped pin fins. Numerical Heat Transfer Applications (Part A). 19 (1991) 381-403.
4. Yang KS, Chu WH, Chen IY, Wang CC. A comparative study of the airside performance of heat sinks having pin fin configurations. International Journal of Heat and Mass Transfer 50 (2007) 661-4667.
5. Sparrow EM, Larson ED. Heat transfer from pin-fins situated in an oncoming longitudinal flow which turns to cross-flow. International Journal of Heat and Mass Transfer 25 (1982) 603-614.
6. Yakut K, Alemdaroglu N, Kotcioglu I, Celik C. Experimental investigation of thermal resistance of a heat sink with hexagonal fins. Applied Thermal Engineering 26 (2006) 2262-2271.
7. Chen Z, Li Q, Meier D, Warnecke HJ. Convective heat transfer and pressure loss in rectangular ducts with drop-shaped pin fins. Heat and Mass Transfer 33 (1997) 219-224.
8. Ricci R, Montelpare S. An experimental IR thermographic method for the evaluation of the heat transfer coefficient of liquid-cooled short pin fins arranged in line. Experimental Thermal and Fluid Science 30 (2006) 381-391.
9. Won SY, Mahmood GI, Ligrani PM., Spatially-resolved heat transfer and flow structure in a rectangular channel with pin fins. International Journal of Heat and Mass Transfer 47 (2004) 1731-1743.
10. Hwang JJ, Lu CC. Lateral-flow effect on end wall heat transfer and pressure drop in a pin-fin trapezoidal duct of various pin shapes. ASME Paper No. 2000-GT-232, 2000.
11. Wang CC, Lo J, Lin YT, Wie CS. Flow visualization of annular and delta winglet vortex generators in fin-and-tube heat exchanger application. International Journal of Heat and Mass Transfer 45 (2002) 3803-3815.
12. Kotcioglu I, Caliskan S, Baskaya S. Experimental study on the heat transfer and pressure drop of a cross-flow heat exchanger with different pin-fin arrays. Heat and Mass Transfer 47 (2011) 1133-1142.
13. Tahat MA, Babus'Haq RF, Probert SD. Forced steady-state convections from pin-fin arrays. Applied Energy 48 (1994) 335-351.
14. El-Sayed SA, Mohamed MS, Abdel-latif AM, Abouda AE. Investigation of turbulent heat transfer and fluid flow in longitudinal rectangular-fin arrays of different geometries and shrouded fin array. Experimental Thermal and Fluid Science 26 (2002) 879-900.
15. Chen TY, Shu TH. Flow structures and heat-transfer characteristics in fan flows with and without delta-wing vortex generators. Experimental Thermal and Fluid Science 28 (2003) 273-282.
16. Jubran BA, Al-Salaymeh AS. Heat-transfer enhancement in electronic modules using ribs and ''film cooling-like'' techniques. International Journal of Heat and Fluid Flow 17 (1996) 148-154.
17. Kline SJ, McClinctock FA. Describing uncertainties in single-sample experiments. Mechanical Engineering 75 (1953) 3-8